Synaptopodin: An Actin-associated Protein in Telencephalic Dendrites and Renal Podocytes

Peter Mundel,* Hans W. Heid,‡ Thomas M. Mundel,* Meike Krüger,* Jochen Reiser,* and Wilhelm Kriz*

*Department of Anatomy and Cell Biology, University of Heidelberg, D-69120 Heidelberg, Germany; and‡Division of Cell Biology, German Cancer Research Center, D-69120 Heidelberg, Germany

Abstract. Synaptopodin is an actin-associated protein of differentiated podocytes that also occurs as part of the actin cytoskeleton of postsynaptic densities (PSD) and associated dendritic spines in a subpopulation of exclusively telencephalic synapses. Amino acid sequences determined in purified rat kidney and forebrain synaptopodin and derived from human and mouse brain cDNA clones show no significant homology to any known protein. In particular, synaptopodin does not contain functional domains found in receptor-clustering PSD proteins. The open reading frame of synaptopodin encodes a polypeptide with a calculated M_r of 73.7 kD (human)/74.0 kD (mouse) and an isoelectric point of 9.38 (human)/9.27 (mouse). Synaptopodin contains a high amount of proline (~20%) equally distributed along the protein, thus virtually excluding the formation of any globular domain. Sequence comparison between human and mouse synaptopodin revealed 84% identity at the protein level.

In both brain and kidney, in vivo and in vitro, synaptopodin gene expression is differentiation dependent. During postnatal maturation of rat brain, synaptopodin is first detected by Western blot analysis at day 15 and reaches maximum expression in the adult animal. The exclusive synaptopodin synthesis in the telencephalon has been confirmed by in situ hybridization, where synaptopodin mRNA is only found in perikarya of the olfactory bulb, cerebral cortex, striatum, and hippocampus, i.e., the expression is restricted to areas of high synaptic plasticity. From these results and experiments with cultured cells we conclude that synaptopodin represents a novel kind of proline-rich, actin-associated protein that may play a role in modulating actin-based shape and motility of dendritic spines and podocyte foot processes.

THE postsynaptic segment of neuronal dendrites consists of the postsynaptic densities (PSD)[1] and the associated dendritic shaft. In the dendritic shaft, an actin-based cytoskeleton is found, which anchors in the PSD (Matus, 1982). It is generally accepted that learning and memory require morphological changes in neurons (for review see Wallace et al., 1991) including remodeling of synaptic contacts. While substantial knowledge about dynamics of axonal filopodia and growth cones in enabling the axon to find its approriate target has accumulated (for review see Bentley and O'Connor, 1994), much less is known about the dynamics of postsynaptic dendritic structures during synaptogenesis and synaptic remodeling. However, recent studies with developing hippocampal slices (Dailey and Smith, 1996) and cultured hippocampal neurons (Papa et al., 1995; Ziv and Smith, 1996) provided evidence for a role of dendritic filopodia in synaptogenesis and spine formation. As in axonal filopodia, the dynamics of dendritic filopodia and spines appear to be mediated, at least in part, by the actin-based cytoskeleton of the dendrites.

Despite the recent progress of the study of the presynaptic proteins, the composition of the PSD and the associated dendritic shaft are still largely elusive (Kennedy, 1993; Garner and Kindler, 1996). However, advances in protein microsequencing and yeast two hybrid system have led to the identification of proteins interacting with the cytoskeleton of the postsynaptic segment. Recently, several members of a novel family of synapse-associated proteins were identified that share the so-called PDZ domain in their NH_2-terminal region, exhibit a guanylate kinase activity, and are homologous to the tight junction-associated protein ZO-1 (for review see Garner and Kindler, 1996; Sheng 1996). These proteins are involved in mediating the clustering of postsynaptic receptors, e.g., of the NMDA receptor as shown by a yeast two hybrid approach

Address all correspondence to Dr. Peter Mundel, Department of Anatomy and Cell Biology, University of Heidelberg, Im Neuenheimer Feld 307, D-69120 Heidelberg, Germany. Tel.: (49) 6221-548687. Fax: (49) 6221-544951. e-mail: peter.mundel@urz.uni-heidelberg.de

1. *Abbreviations used in this paper*: aa, amino acid; CNS, central nervous system; MAP, microtubule-associated protein; ORF, open reading frame; PSD, postsynaptic densities.

(Kornau et al., 1995). On the other hand it has been found that NCAM-180, ankyrin, and a membrane-bound ankyrin-binding protein are involved in linking spectrin and α adducin to the microfilament system of the postsynaptic segment (summarized in a model by Garner and Kindler, 1996). One possible candidate for providing the missing link between the receptor(s) and the actin filament system (the activity of the NMDA receptor is dependent on the integrity of actin [Rosenmund and Westbrook, 1993]) appears to be α actinin-2, which was shown to bind the NMDA receptor in competition with calmodulin (Wyszynski et al., 1997).

Podocytes of the renal glomerulus are unique cells with a complex cellular organization. With respect to their cytoarchitecture, podocytes may be divided into three structurally and functionally different segments: cell body, major processes, and foot processes. In the foot processes a complete microfilament-based contractile apparatus is present, which is composed of actin, myosin II, α actinin, talin, and vinculin (Drenckhahn and Franke, 1988). The linkage of this system to the glomerular basement membrane at focal contacts is mediated by an $\alpha_3\beta_1$ integrin complex (Adler, 1992). Like the PSD, the sole plate of podocyte foot processes contains an amorphous density, which in its molecular composition is largely unknown (for review see Mundel and Kriz, 1995). Podocytes are known to respond to a variety of vasoactive substances with changes of their cytoskeleton (Mundel and Kriz, 1995) and are able to perform slow and directed movements of their foot processes (Shirato et al., 1996).

In a previous study, we described the association of a protein defined by mAb G1 with the actin system of podocyte foot processes (Mundel et al., 1991). We now report on the molecular characterization of this protein, which we termed synaptopodin, since, in addition to renal podocytes, it is expressed in the brain, where it associates with the actin cytoskeleton of PSD and dendritic spines in a subset of telencephalic synapses. We discuss the potential role of synatopodin in modulating the actin-based motility of podocyte foot processes and telencephalic dendritic spines.

Materials and Methods

Tissues for Immunohistochemistry

Female adult Sprague-Dawley rats (BW 200g) were perfused via the abdominal aorta with 2% paraformaldehyde in PBS for 3 min at 220 mm Hg followed by cryoprotectant sucrose-PBS solution (800 mOsmol) for 5 min at 220 mm Hg. Organs were harvested and slices of tissues were frozen in isopentane cooled by liquid nitrogen to −160°C. In addition to kidney and brain the following organs were analyzed: liver, heart, lung, skeletal muscle, adrenal gland, testis, salivary glands, stomach, pancreas, spleen, small intestine, and colon.

Hippocampal Cultures

Cultures of hippocampal cells were prepared from the brains of 18-d-old fetal Sprague-Dawley rats exactly as described (Cid-Arregui et al., 1995). Briefly, after chemical and mechanical dissociation of the hippocampi, cells were plated onto polylysine-coated glass cover slips (15-mm diam). These neurons survive and undergo full polarization when cultured in serum-free medium in the presence of a supporting layer of astrocytes (Goslin and Banker, 1991).

Podocyte Cultures

Adult podocyte cell lines were cloned by limiting dilution from glomerular cultures of the "immortomouse" (Jat et al., 1991) harboring a transgene for a thermosensible variant of the SV-40-T–antigen, which is under the control of the H-2K^b-promotor, whose activity can be increased by γ interferon. The cellular origin of the cloned cell lines from the podocyte lineage was proven by the detection of the Wilm's tumor gene product (WT-1), which in the adult kidney is an exclusive marker of podocytes (Mundlos et al., 1993). Cells were propagated at 33°C in RPMI 1640 containing 10% FCS (Boehringer Mannheim, Mannheim, Germany), 100 U/ml penicillin (GIBCO BRL, Karlsruhe, Germany), 100 μg/ml streptomycin (GIBCO BRL), and 10 U/ml recombinant mouse γ interferon (Sigma Chemical Co., Munich, Germany) to induce synthesis of the immortalizing T antigen. Subcultivation was done with trypsin at 37°C after cells had reached confluence. Cells were passaged after 1:5 dilution. To initiate differentiation, cells were thermoshifted to 37°C and maintained in medium without γ interferon (Mundel et al., 1997).

Depolymerization Studies

These experiments were carried out with differentiated arborized podocytes after 7 to 14 d at 37°C. Cells were treated for different time intervals (3, 6, and 24 h) with actin-depolymerizing cytochalasin B (0.4–10 μm) and microtubule-depolymerizing colcemid (0.5 μM). At different time points after drug treatment, cells were prepared for immunofluorescence labeling. To study the reversibility of alterations, the drugs were removed, and cells were washed twice with RPMI 1640 and allowed to recover for different time intervals before preparation for immunocytochemistry.

Antibodies

Synaptopodin-specific Antibodies. The generation and initial characterization of anti-synaptopodin mAb G1 has been described previously (Mundel et al., 1991). Polyclonal antisera were obtained by immunization of rabbits with keyhole limpet hemocyanin-conjugated peptides. The antisera were affinity purified with the corresponding peptides linked to Ultralink (Pierce, Sankt Augustin, Germany) according to the manufacturer's instructions. In the experiments described in this manuscript, antiserum 26-1E directed against the sequence of amino acid (aa) 441–455 corresponding to rat brain synaptopodin peptide fragment No. 26 (which is identical to rat glomerular synaptopodin peptide fragment No. 25; single letter code SPGAAAEETVPEWASC) and antiserum NT-61 directed against aa 181–195 of mouse brain synaptopodin corresponding to aa 188–202 of human brain synaptopodin (single letter code MSSLLIDMQPSTLV) were routinely used.

Additional Primary Antibodies. Rabbit anti-synaptophysin (DAKO, Hamburg, Germany), rabbit anti–MAP2 (Boehringer Mannheim), rabbit anti-β tubulin (Sigma Chemical Co.), rabbit anti–WT-1 (C19; Santa Cruz Biotechnology, Heidelberg, Germany), monoclonal anti-vinculin (Sigma Chemical Co.), and rhodamine-conjugated phalloidin (Sigma Chemical Co.) to detect F-actin.

Immunofluorescence Microscopy

Immunofluorescence staining was routinely performed on 4-μm, frozen sections from rat kidney and 8-μm, frozen sections from rat brain as well as with cultured rat hippocampal neurons growing on poly-lysine–coated coverslips after 25 d in vitro and with cloned mouse podocytes growing on collagen type I–coated glass cover slips. To test for additional expression of synaptopodin, sections from the following organs were analyzed by immunohistochemistry: liver, heart, lung, skeletal muscle, adrenal gland, testis, salivary gland, stomach, pancreas, spleen, small intestine, and colon (cytosolic extracts from these organs were also analyzed by immunoblotting; see below). Cultured cells were either fixed with ice-cold acetone at −20°C for 5 min or with 2% paraformaldehyde and 4% sucrose in PBS for 5 min followed by permeabilization with 0.3% Triton X-100 in PBS for 5 min at room temperature. After rinsing with PBS, unspecific binding sites were blocked with 2% FCS, 2% BSA, and 0.2% fish gelatine in PBS for at least 30 min. Primary antibodies (prediluted in blocking solution) were applied for 60 min at room temperature. Antigen–antibody complexes were visualized using fluorochrome (Cy2 or Cy3)-conjugated secondary antibodies (Biotrend, Cologne, Germany). Sections were washed with PBS, rinsed with H_2O, and mounted in 15% Mowiol (Calbiochem, Bad Soden, Germany) and 50% glycerol in PBS. After overnight drying, speci-

mens were analyzed and documented with a photomicroscope (Polyvar 2; Leica, Bensheim, Germany). Simultaneous confocal double fluorescence microscopy was done with a laser scanning microscope (410 UV; Carl Zeiss, Oberkochen, Germany) with appropriate filters. Micrographs were taken with an imagecoder (Focus Graphics, Foster City, CA) or printed with a sublimation video printer.

Immunoelectron Microscopy

For preembedding immunoperoxidase labeling, cryostat sections of perfusion-fixed tissues from rat brain were cut at 20 μm and processed as free-floating sections. After preincubation in PBS containing 10% normal swine serum, synaptopodin mAb G1 (prediluted 1:16 in PBS containing 10% normal swine serum) was applied overnight at room temperature, followed by biotinylated donkey anti–mouse IgG (1:50) for 1 h. After washing with PBS, sections were placed in streptavidin-conjugated peroxidase complexes (1:200). Peroxidase activity was detected using 3,3′-diaminobenzidine as chromogen. The sections were stained en bloc with uranyl acetate in maleate buffer, osmicated in 1% OsO_4 for 1 h, dehydrated in graded series of acetone, and flat embedded in epon between teflon-coated slide and coverglass. Areas of interest were selected under a light microscope, excised with a razor blade, and mounted onto preformed epon blocks. Thin sections were cut with an ultramicrotome E (Leica) and examined under a Philips EM 301.

Tissue Fractionation and Protein Extraction for Immunoblotting and Protein Purification

Brains and kidneys from 20 adult Sprague-Dawley rats (body mass 200 g) were harvested. Dissected forebrains and cerebella were immediately frozen in liquid nitrogen. Isolation of glomeruli from kidneys was done by passing tissue through a series of steel sieves exactly as described (Mundel et al., 1991). Samples were stored at −80°C until used.

Protein extraction was carried out at 4°C in a tight-fitting Potter homogenizer with 15 strokes at 1,300 rpm in 10 vol of homogenization buffer (20 mM Tris, 500 mM NaCl, pH 7.5) supplemented with 0.5% Chaps (Sigma Chemical Co.), 5 mM EDTA, and the following protease inhibitors (all from Serva, Heidelberg, Germany): 2 μm Pepstatin, 2 μm Leupeptin, and 200 μm Pefabloc. Insoluble material was pelleted at 50,000 *g* for 30 min at 4°C. The resulting crude supernatants (C-Sup) were stored at −20°C or further processed to obtain heat-stable protein fractions (Herzog and Weber, 1978). To this end, the concentration of NaCl was adjusted to a final concentration of 800 mM, and 5% 2-mercaptoethanol was added. The samples were boiled for 5 min and insoluble material was pelleted at 50,000 *g* for 30 min at 4°C. The resulting heat-stable supernatants (HS-Sup) were stored at −20°C until used.

For the analysis of synaptopodin expression during postnatal maturation of the brain, C-Sups were prepared from rat forebrains and cerebella harvested at day 5, 10, 15, 20, and 50 postnatal. At each time point material from five animals was pooled.

Gel Electrophoresis, Immunoblotting, and Protein Sequence Analysis

C-Sups and HS-Sups from isolated glomeruli, forebrain, and cerebellum were diluted with SDS sample buffer, boiled for 5 min, and separated on 8% SDS polyacrylamide gels. Proteins were transferred to Immobilon P membranes (Millipore Corp., Eschborn, Germany) by semidry blotting and stained with 0.05% Coomassie brilliant blue in 40% methanol and 7% acetic acid. Before immunodetection, the membranes were destained with 50% methanol and 2% acetic acid. Primary antibodies (either hybridoma supernatant of mAb G1 or affinity-purified polyclonal antibodies 26-1E and NT-61) were used at 1:500 to 1:2,000, and horseradish peroxidase-conjugated secondary antibodies (Promega, Heidelberg, Germany) were used at 1:20,000. The immunoreaction was visualized by chemiluminescence (Amersham Intl., Braunschweig, Germany) and film exposure. To test for possible expression of synaptopodin in other organs than brain and kidney, cytosolic extracts from a variety of organs (liver, heart, lung, skeletal muscle, adrenal gland, testis, salivary glands, stomach, pancreas, spleen, small intestine, and colon) were analyzed by immunoblotting.

For protein sequencing, synaptopodin was enriched from rat forebrain and from isolated glomeruli by preparative HPLC-reversed phase chromatography, and purification steps were monitored by Western blotting using mAb G1 to detect the protein. Per run, 5 ml of HS-Sup (see above) were loaded onto a Brownlee 4.6-mm C8 column (Applied Biosystems, Weiterstadt, Germany) and developed with a linear gradient of 10 to 80% acetonitrile during 45 min. To avoid contaminations, different columns were used for the separation of brain and glomerular extracts. 1-ml fractions were collected; 100-μl aliquots were lyophylized, resuspended in SDS sample buffer, and analyzed by immunoblotting. Positive fractions were lyophylized, resuspended in 100 μl of lysis buffer, and separated by two-dimensional gel electrophoresis with NEPHGE (non-equilibrium pH gradient gel electrophoresis) in the first dimension, followed by separation in 8% SDS gels in the second dimension as described (Heid et al., 1994). After transfer to Immobilon P membranes, protein spots were excised from Coomassie brilliant blue-stained membranes. Tryptic digestions of excised spots, HPLC separations of resulting internal peptide fragments, and peptide microsequencing were done as described (Heid et al., 1994), except that Edman degradation was carried out on a protein sequencing apparatus (Procise 494; Applied Biosystems).

cDNA Cloning and Sequencing

Data base searches identified three expressed sequence tag (EST) clones obtained from Research Genetics (Huntsville, AL) termed sp17 (these sequence data available from EMBL/GenBank/DDBJ under accession number H49442), sp47 (accession number R88417), and sp91 (accession number R90893) orientated from 5′ to 3′, with clone sp17 containing a "Kozak sequence" (Kozak, 1989) before the start codon and clone sp91 ending with a polyA-tail (from a human brain cDNA library that covered the open reading frame [ORF] of human synaptopodin, except for a gap of 250 bases between clone sp47 and sp91). This gap was filled after reverse transcription of human hippocampal RNA into cDNA by PCR cloning using specific primers deduced from the sequences of clones sp47 and sp91, respectively. The region spanning the ORF was sequenced in both directions, using internal oligonucleotide primers.

The mouse homologue of the synaptopodin gene product was cloned by a combination of cDNA library screening and RT-PCR cloning. To this end, a mouse brain cDNA library (λTriplEx; Clontech, Heidelberg, Germany) was screened under low stringency conditions using clones sp17 and sp47 as probes. Among several shorter clones, one clone (termed 7A-1) was obtained, which covers the region between bp 490 and the poly A tail of mouse brain synaptopodin cDNA. The first 489 bp of the ORF were cloned by nested RT-PCR from random-primed mouse brain cDNA using two specific 3′ primers derived from the 5′ region of clone 7A-1 and one degenerate primer corresponding to bp 1–25 of the human synaptopodin ORF. With this approach, the complete ORF of mouse brain synaptopodin was established.

Sequence alignments, analyses, and data base searches were done with the software program package HUSAR (Heidelberg Unix Sequence Analysis Resources).

RNA Isolation and Northern Blot Analysis

Total RNA was isolated from human brain cortex and hippocampus, from rat brain forebrain and cerebellum, and from rat kidney cortex using the RNeasy total RNA kit (Quiagen, Hilden, Germany) according to the manufacturer's instructions. Northern blot analyses were done as described (Schäfer et al., 1994), with ^{32}P-labeled antisense riboprobes using clone sp47 as a template. Equal RNA loading was confimed by hybridization with a GAPDH-riboprobe.

In Situ Hybridization Studies

Radioactive in situ hybridization of sagittal and coronal frozen sections from adult mouse brain was carried out as described by Monyer et al. (1992) using ^{35}S-labeled antisense oligonucleotides derived from the region between bp 600 and 800 of mouse brain synaptopodin cDNA. Exposure time to Kodak XAR-5 film was 24 d.

Results

Biochemical Analysis of Synaptopodin

Using mAb G1, a heat-stable protein with an apparent molecular mass of 100 kD was recognized by immunoblotting in cytosolic extracts from rat brain (Fig. 1). In cytosolic fractions from isolated rat kidney glomeruli, a heat-stable band with an apparent molecular mass of 110 kD was shown

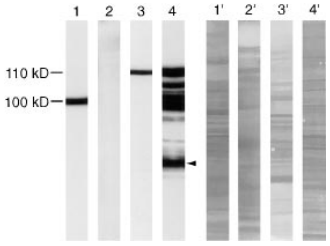

Figure 1. Western blot analysis of synaptopodin with mAb G1. Lanes *1–4* show the immunodetection; lanes *1′–4′* show staining of the identical membrane with Coomassie brilliant blue to demonstrate protein loading and separation. Cytosolic extracts from rat forebrain (lane *1*), cerebellum (lane *2*), and isolated glomeruli (lanes *3* and *4*) were analyzed in parallel. While in the forebrain a protein of ~100 kD is present, no protein expression is seen in cerebellum. In kidney a 110-kD band is observed. The extract in lane *4* had been kept at 4°C for 24 h before separation. Several proteolytic fragments appear; the band indicated by an arrowhead represents the originally described 44-kD protein.

(Fig. 1). The originally described 44-kD band (Mundel et al., 1991) represents a proteolytic fragment of the 110-kD protein (Fig. 1). On two-dimensional gel electrophoresis, synaptopodin appeared as a very basic protein with an isoelectric point around 9.4 (Fig. 2).

A polyclonal antiserum (26-1E), directed against an internal aa sequence corresponding to rat brain synaptopodin peptide fragment No. 26 (which is identical to rat kidney peptide fragment No. 25; see below), recognized the 110-kD band in glomerular extracts and the 100-kD band in cytosolic extracts from rat and human brain as originally described mAb G1. A second polyclonal antibody (NT-61) directed against a peptide sequence located in the 5′ region of mouse brain synaptopodin identifies the same 110/100-kD bands in kidney/brain cytosolic extracts (data not shown).

To examine the solubility of synaptopodin, fractionation experiments of rat forebrain were carried out. In low salt (150 mM NaCl) buffer, only a partial extraction of synaptopodin was achieved, whereas homogenization with high salt (500 mM NaCl) buffer supplemented with 0.5% Chaps resulted in complete extraction of the protein (data not shown).

Purification and Peptide Sequencing of Rat Brain and Kidney Synaptopodin

Synaptopodin was purified from rat kidney glomeruli and forebrain. Protein bands were cut from preparative two-dimensional blots and subjected to tryptic digestion. 20 of the resulting internal peptides of the brain protein were analyzed by Edmann degradation. Data base comparison revealed that five peptides matched with two EST clones (clones sp47 and sp91) from a human brain cDNA library. A third EST clone from the same library (clone sp17) was identified by overlapping with the 5′-end of clone sp47. To prove the identity of the renal and the brain protein, six peptide fragments of the purified glomerular protein were subjected to Edmann degradation. All of these peptide fragments revealed identical aa composition as the correponding peptide fragments of the brain protein (Fig. 3).

Cloning and Sequencing of Synaptopodin cDNA

The complete cDNA sequence of human brain synaptopodin was established from three EST clones (termed sp17, sp47, and sp91) and an additional fragment that covered a 250-b gap between clones sp47 and sp91, which was obtained by RT-PCR cloning. While clone sp17 contained a consensus sequence for initiation of translation, clone sp91 contained ~2.1-kB 3′-untranslated sequence and ended with a consensus site for polyadenylation (data not shown). The deduced protein sequence codes for a 685-aa polypeptide with a calculated M_r of 73.7 kD and an isoelectric point of 9.38 (Fig. 3 *a*). Molecular cloning of the mouse homologue of synaptopodin revealed an ORF of 2,071 bp and additional 1,500-bp 3′-untranslated region. The ORF codes for a 690-aa protein with a calculated M_r of 74.0 kD and an isoelectric point of 9.27 (Fig. 3 *b*). At the protein level an identity of 84% was found between human and mouse.

We performed Northern blots with RNA from human

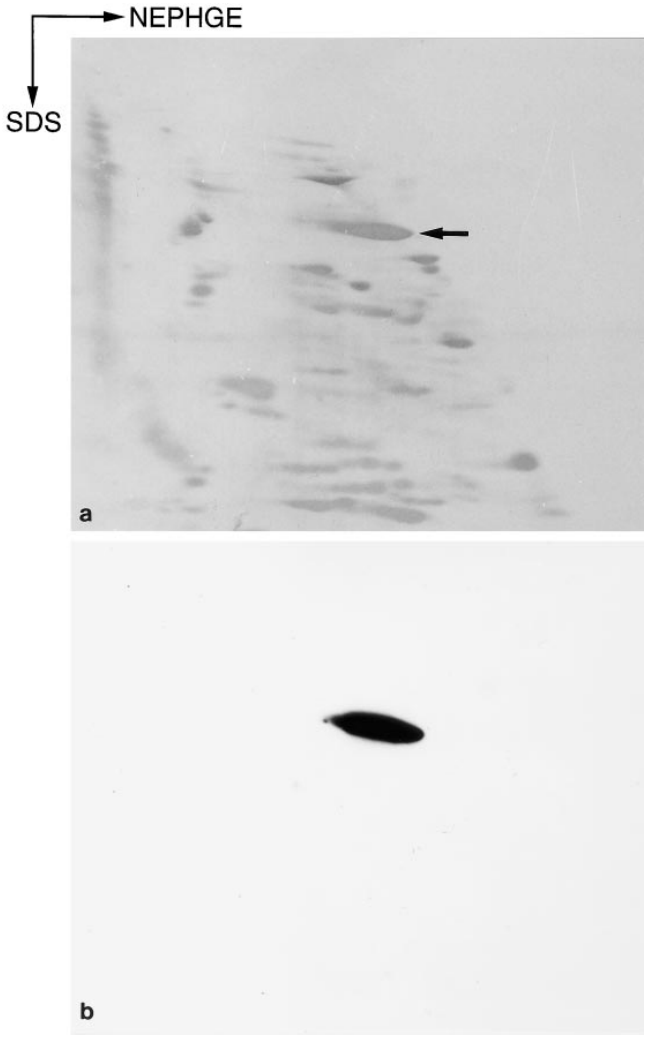

Figure 2. Two-dimensional analysis of rat brain synaptopodin. (*a*) Coomassie brilliant blue-stained two-dimensional Western blot, using NEPHGE in the first dimension and SDS-PAGE in the second, of a fraction enriched for synaptopodin (*arrow*) obtained after reversed-phase HPLC chromatography of a heat-stable supernatant from rat forebrain cytosolic extracts. (*b*) ECL detection of synaptopodin using mAb G1.

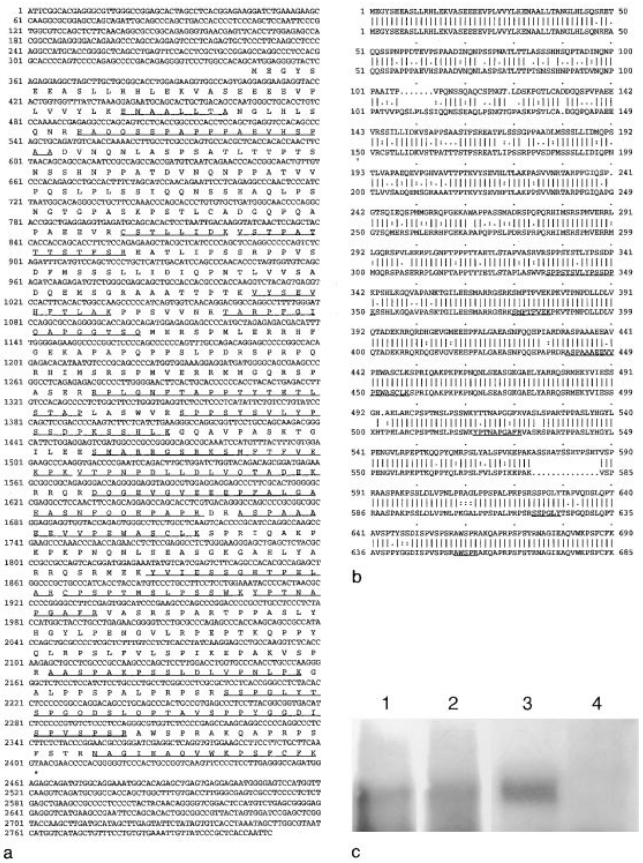

Figure 3. (*a*) Nucleotide sequence (*upper lines* and *numbers*) and deduced amino acid sequence (*one letter code*, *lower lines*, and *numbers*) of human brain synaptopodin cDNA. Taking the first possible start codon of the open reading frame, synaptopodin consists of 685 aa. aa sequences determined by Edman degradation of proteolytically derived internal peptides of rat brain synaptopodin are underlined. (*b*) Comparison of the aa sequences between mouse (*upper lines*) and human (*lower lines*) synaptopodin. At the protein level an 84% identity between the two species is observed. aa sequences determined from internal peptides of rat kidney synaptopodin are underlined. The sequence data of human synaptopodin are available from EMBL/GenBank/DDBJ under accession number Y11072. (*c*) Northern blot analysis of synaptopodin. A single 4.4-kbp mRNA is detected in human brain cortex (*1*), in rat kidney cortex (*2*), and rat forebrain (*3*). No signal is obtained in rat cerebellum (*4*).

cerebral cortex, rat forebrain, and cerebellum as well as from rat kidney cortex, using a riboprobe derived from clone sp47. While in rat cerebellum no signal was obtained, in each of the other tissues, a single 4.4-kB transcript was detected after overnight exposure (Fig. 3 *c*), with this confirming the immunoblotting and immunohistochemical results.

On sequence comparison, synaptopodin shows no significant homology to any published proteins. Due to its high content of proline (~20%) evenly distributed along the protein, no formation of any globular domain is possible. In addition to several potential phosphorylation sites spread throughout the molecule, synaptopodin contains two PPXY motifs (corresponding to aa 318–321 and 337–340 of the human protein; Fig. 3 *a*), which are also found in the mouse protein (aa 310–313 and 329–332; Fig. 3 *b*). These PPXY motifs are involved in protein–protein interactions between proteins bearing proline-rich peptide stretches and the WW domain of a variety of proteins (Einbond and Sudol, 1996).

Synaptopodin Expression in Kidney and Brain

To see whether synaptopodin is expressed by other organs than kidney and brain, we performed immunohistochemical stainings as well as Western blot analyses of a variety of organs (for details see Materials and Methods). All tissues examined did not show any synaptopodin reactivity with either technique, i.e., synaptopodin is restricted to kidney and brain (data not shown).

Distribution of Synaptopodin in the Brain

To determine the distribution of synaptopodin in the brain, we performed immunofluorescence stainings of sagittal and coronal serial sections of the adult rat brain. Synaptopodin was found in the olfactory bulb, the cerebral cortex, the striatum, and the hippocampus (Fig. 4). The immunoreactivity was observed in the dendritic layers, whereas the perikarya were free of labeling. No other regions of the central nervous system (CNS) showed any expression of synaptopodin as confirmed by additional immunohistochemical mapping of serial coronal sections from a complete rat brain using the preembedding peroxidase technique (data not shown). Applying the polyclonal antisera NT-61 and 26-1E, the same pattern of immunoreactivity was observed as with the original mAb G1 (data not shown). Within the striatum, synaptopodin expression was restricted to the telencephalic part, i.e., the putamen, whereas the globus pallidum, which belongs to the diencephalon, was not reactive with anti-synaptopodin antibodies (Fig. 5). To reveal the subcellular localization of synaptopodin, we performed preembedding PAP labeling experiments of telencephalic regions that had been found to express synaptopodin. The electron-dense reaction product was restricted to postsynaptic densites and associated dendritic spines of a subset of synapses (Fig. 6). While the PSD itself was homogeneously decorated with the DAB reaction product (Fig. 6, *a* and *b*), in the adjacent dendritic shaft a clustered arrangement of the immunoreactivity was observed (Fig. 6, *c* and *d*). The restriction of synaptopodin expression to a subset of synapses was confirmed by a double immunofluorescence labeling approach with mAb G1 for synaptopodin and polyclonal anti-synaptophysin antiserum as a marker of all synapses (Fig. 7).

The distribution pattern of synaptopodin was corroborated by in situ hybridization studies showing that synaptopodin mRNA was present in the olfactory bulb, cerebral cortex, striatum, and hippocampus; expression was only observed in perikarya but not in dendritic layers (Fig. 8). Thus, as shown before by immunohistochemistry, within the CNS, synaptopodin indeed is restricted to the telencephalon.

Expression of Synaptopodin during Postnatal Maturation of Rat Brain

To examine the maturation-dependent expression of synaptopodin during brain development, we analyzed cyto-

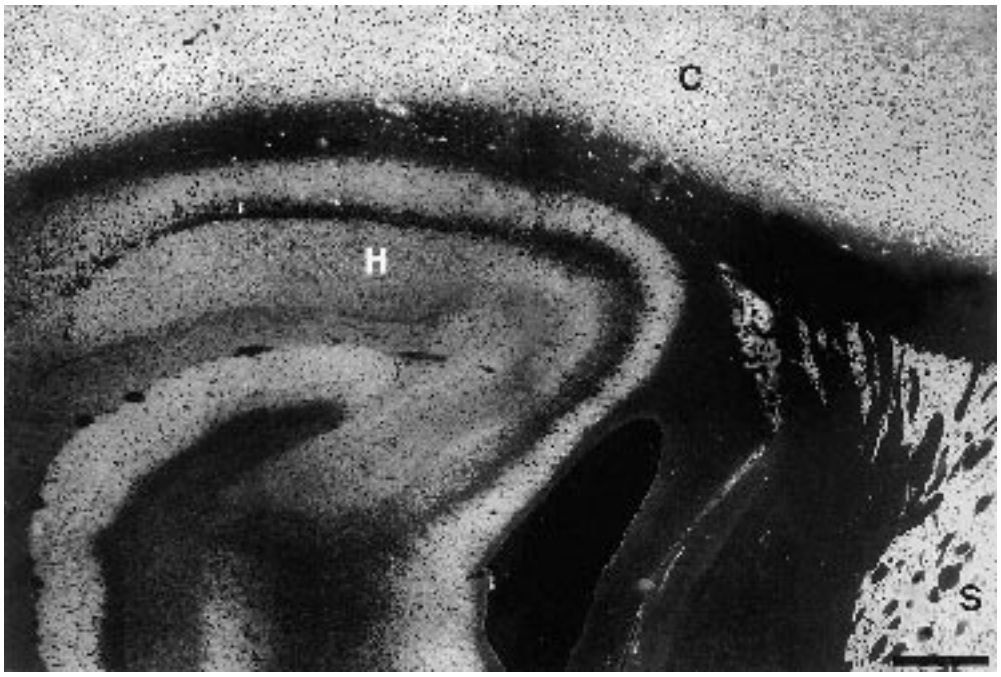

Figure 4. Overview of synaptopodin staining in rat forebrain. The distribution of synaptopodin in adult rat brain was analyzed by indirect immunofluorescence labeling of 8-μm–thick frozen sections from perfusion-fixed tissue. This frontal section through the forebrain reveals expression in the cerebral cortex (*C*), striatum (*S*), and hippocampus (*H*). The protein was also found in the olfactory bulb (not shown). No other areas of the central nervous system show any synaptopodin expression.

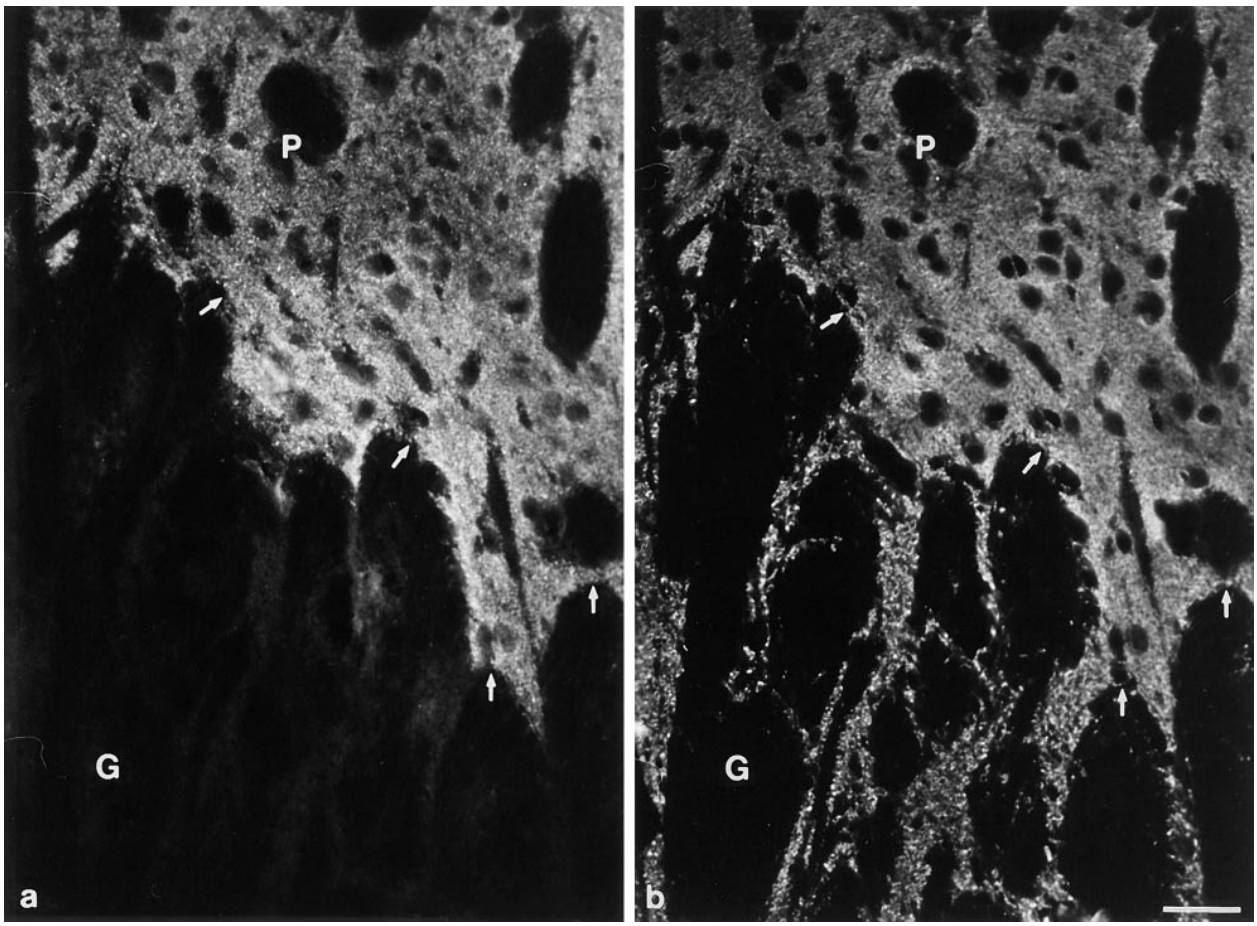

Figure 5. Immunofluorescence microcopy of synaptopodin in striatum. This micrograph shows the transition between the telencephalic putamen (*P*) and the diencephalic globus pallidum (*G*). (*a*) Synaptopodin staining is restricted to the putamen and ends at the border to the diencephalon (*arrows*). (*b*) Staining with anti-synaptophysin to detect all synapses. Bar, 1.5 μm.

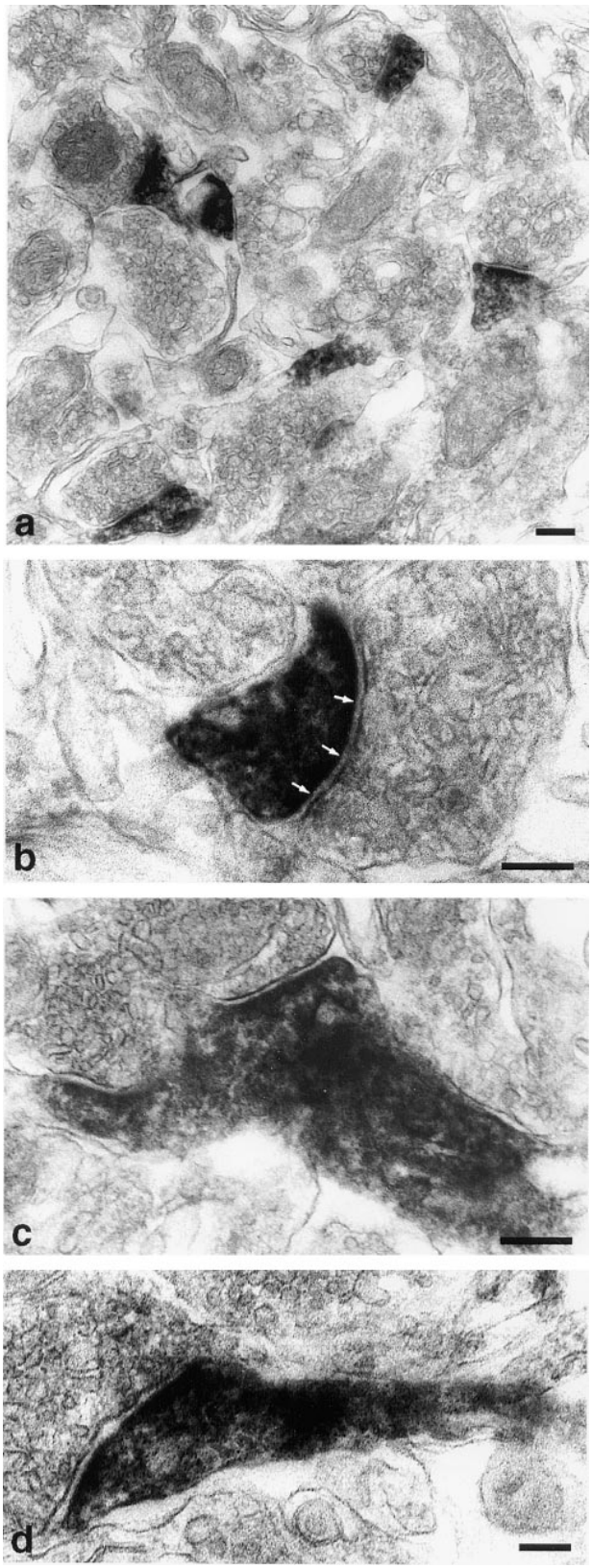

Figure 6. Immunoelectron microscopic analysis of synaptopodin. The subcellular localization of synaptopodin in the telencephalon was analyzed by preembeding peroxidase labeling. (*a*) The electron-dense reaction product localizes to the postsynaptic densities and dendritic spines of distinct synapses. (*b*) At a higher magnification the strongest labeling is found at the PSD (*arrows*). (*c* and *d*) Extension of synaptopodin expression into dendritic shaft. This distribution of synaptopodin in the postsynaptic segment of dendrites corresponds exactly to the distribution of actin at this site. Bars, 0.2 μm.

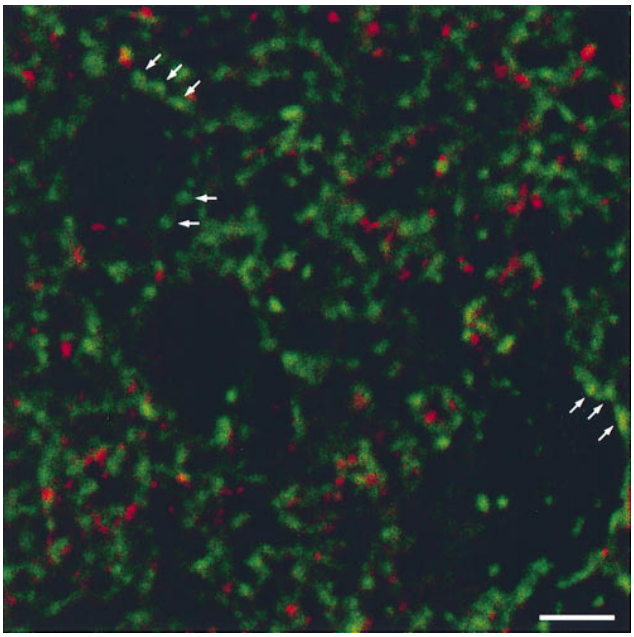

Figure 7. Confocal laser scanning double fluorescence analysis of synaptopodin and synaptophysin in rat brain striatum. In contrast to synaptophysin (*green*), which is expressed in all synapses, synaptopodin (*red*) is only expressed by a subpopulation of synapses. It becomes evident that axosomatic synapses (*arrows*) are virtually free of synaptopodin immunoreactivity. Bar, 10 μm.

solic extract from rat forebrains and cerebella at postnatal days 5, 10, 15, 20, and 50 by Western blotting. Synaptopodin was first expressed around day 15, increased thereafter, and reached the maximum level of expression in the adult brain (Fig. 9). Like in the adult brain, no expression of synaptopodin was observed in the cerebellum during postnatal maturation. To prove equal protein loading, blot membranes were probed with anti-tubulin antibody and showed comparable signal intensity in all lanes (data not shown).

Immunofluorescence Microscopy of Cultured Hippocampal Neurons

We next analyzed the expression of synaptopodin in cultured neurons derived from embryonic 18-d-old rat hippocampi. The expression started at day 12 in vitro, increased thereafter in parallel with process and spine formation, and reached its maximum expression after 25 d in vitro (Fig. 10 *a*). Like in vivo, synaptopodin was only found in dendrites as revealed in double labeling experiments with anti-MAP2 (Fig. 10 *c*). The immunofluorescence signal was arranged in a dotted pattern along the dendrites, with the dots corresponding to synapses as demonstrated in double labeling experiments with anti-synaptophysin (Fig. 10 *d*).

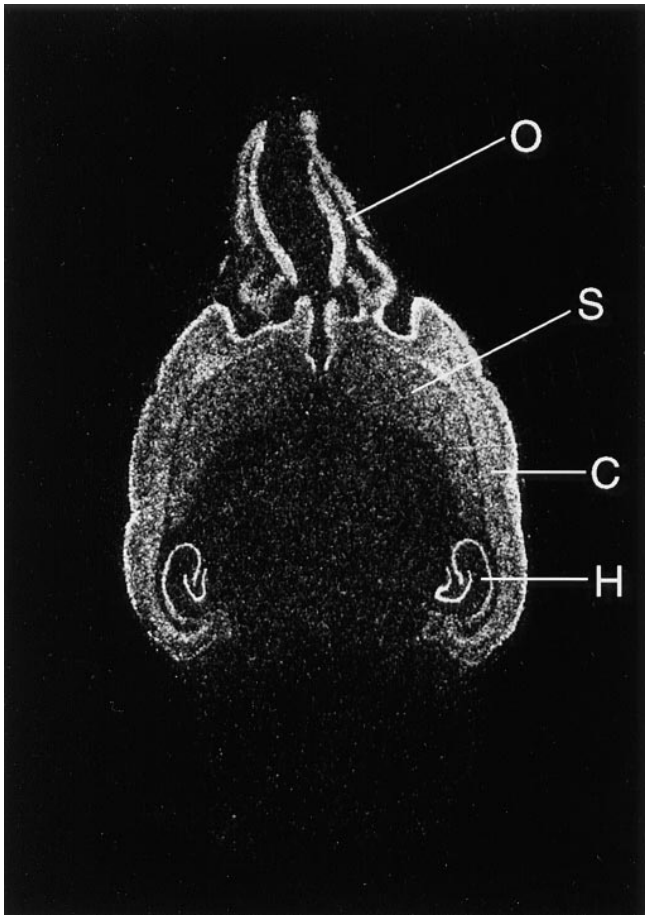

Figure 8. Regional distribution of synaptopodin mRNA in mouse brain. The signal is found in the olfactory bulb (*O*), cortex cerebri (*C*), striatum (*S*), and hippocampus (*H*). This expression pattern matches the immunohistochemical distribution of the protein.

Immunofluorescence Microscopy of Cultured Podocytes

The association of synaptopodin with actin was further analyzed in a conditionally immortal podocyte cell line recently established in our laboratory (Fig 11; Mundel et al., 1997). This cell line can be maintained in two different phenotypes, as undifferentiated cobblestones growing as an epithelial monolayer (Fig. 11 *a*) and as differentiated, arborized cells equipped with processes (Fig. 11 *b*); these arborized podocytes always arise by conversion from cobblestones.

In cultured podocytes, synaptopodin was not found in undifferentiated cobblestones lacking processes (Fig. 11 *c*) but was induced during process formation and showed strongest labeling in differentiated, arborized cells, where it was found in a dotted pattern along the actin microfilaments and in focal contacts (Fig. 11 *d*). The presence in focal contacts was confirmed in double labeling experiments with vinculin (data not shown).

The association with actin (Fig. 11 *e*) was confirmed in double labeling experiments with phalloidin (Fig. 11 *f*). Depolymerization of F-actin with cytochalasin B resulted in a redistribution of synaptopodin in a coarse perinuclear pattern being reversible after washing out of cytochalasin B (Fig. 11 *g*). Depolymerization of the microtubular network with colcemid did not significantly affect the distribution pattern of synaptopodin (Fig. 11 *h*). These results demonstrate that synaptopodin is intimately associated with actin, corroborating the biochemical findings that complete solubilization of synaptopodin requires high salt (500 mM NaCl) buffer.

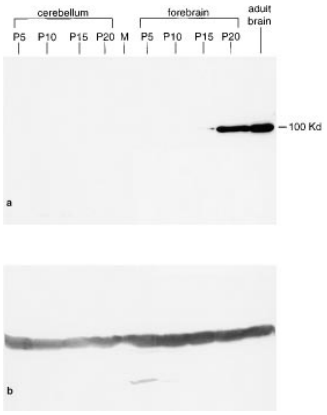

Figure 9. Maturation-dependent expression of synaptopodin during postnatal development of rat brain. (*a*) Cytosolic extracts from cerebellum and forebrain harvested at day 5, 10, 15, and 20 postnatal and from adult rats were analyzed by Western blotting. In the cerebellum, synaptopodin was never expressed. In the forebrain, synaptopodin first appeared around day 15, increased thereafter, and reached the maximum level of expression in the adult animal. (*b*) The identical membrane was probed with anti-tubulin to prove equal protein loading in all lanes.

Discussion

In the present study we have cloned and characterized synaptopodin, which constitutes a novel class of polypeptides in renal podocytes and telencephalic dendrites. Based on its aa composition and tissue distribution, synaptopodin is different from all other actin-associated proteins described so far. Synaptopodin is a rather basic protein with a calculated molecular mass of 73.7 kD (human)/74.0 kD (mouse) and an isoelectric point of 9.38 (human)/9.27 (mouse). The difference between calculated mass and the molecular weight determined by SDS-PAGE and Western blot as 100 kD may be attributed to either posttranslational modifications or may be the consequence of the high content of proline leading to a relative mobility shift in the gel.

Synaptopodin extracted from kidney glomeruli shows a slightly higher M_r of 110 kD than the 100-kD protein from brain, as revealed by Western blot analysis. The reason for this difference remains to be established. However, for several reasons this difference appears to be due to posttranslational modifications, most likely the consequence of differential phosphorylation (as is the case for VASP [vasodilator-stimulated phosphoprotein], another proline-rich, actin-associated protein; see below). First, by Northern blot analysis, one single band with an approximate size of 4.4 kb, was found in rat kidney cortex as well as in rat forebrain and human brain cortex, ruling out the generation of different isoforms by alternative splicing. Second, the internal peptide pattern obtained by tryptic digestion of both the renal and the neuronal protein, resulted in very similar HPLC profiles; all peptide sequences determined from the glomerular protein were identical to corresponding sequences obtained from the brain protein. Third, two polyclonal antisera directed against two internal peptide sequences determined from brain synaptopodin recog-

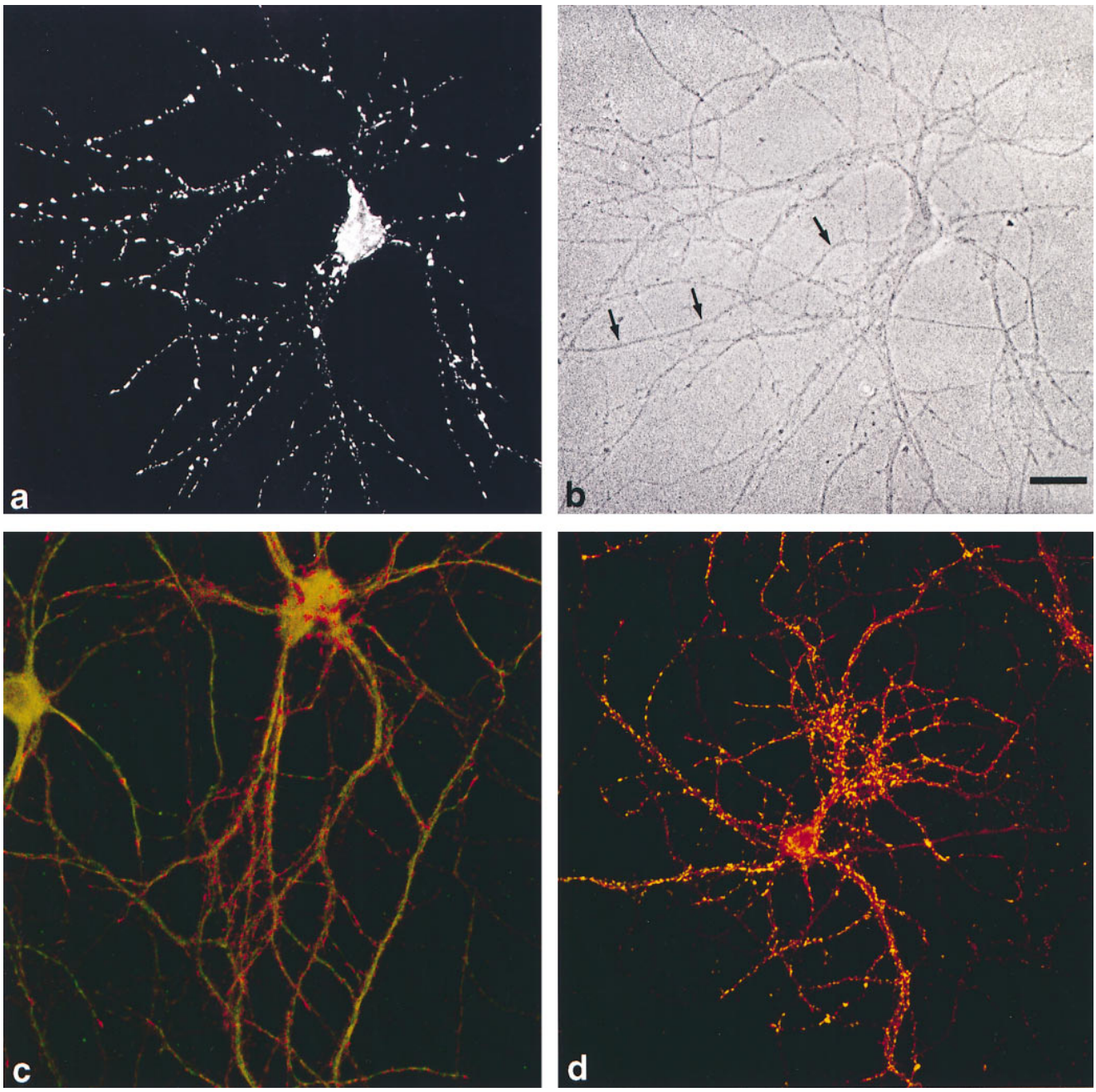

Figure 10. Expression of synaptopodin in cultured hippocampal neurons. (*a*) In 25-d-old cultured hippocampal neurons, a dotted pattern of immunoreactivity in dendrites is seen, whereas axons (*arrows*) are not labeled. (*b*) Phase contrast microscopy. (*c*) Confocal laser scanning double fluorescence analysis of synaptopodin (*red*) and MAP2 (*green*) to demonstrate the exclusive expression of synaptopodin in dendrites. (*d*) Confocal laser scanning double fluorescence analysis of synaptopodin and synaptophysin. The yellow signal results from a complete overlap of the immunoreactivity and proves the synaptic localization of synaptopodin in cultured neurons. Bar, 10 μm.

nized the 110-kD protein in kidney and the 100-kD protein in brain. One of these antibodies, 26-1E, was generated against an aa sequence in the central part of the neuronal form that is identical to the corresponding peptide fragment of the renal protein. The other antibody, NT-61, was generated against an aa sequence deduced from the NH_2-terminal portion of the mouse brain ORF.

In contrast to the brain, in kidney, high concentrations of proteolytic enzymes are present, and like proline-rich proteins in general, synaptopodin is very susceptible to proteolytic degradation. In an extract containing high concentrations of several protease inhibitors (for details see Materials and Methods) that had been kept for 24 h at 4°C before boiling with SDS sample buffer, several proteolytic fragments appeared; one of the major fragments represents the originally described 44-kD protein (Mundel et al., 1991). However, this degradation can effectively be prevented by boiling with SDS sample buffer immediately after protein extraction.

Due to its high content of proline evenly distributed

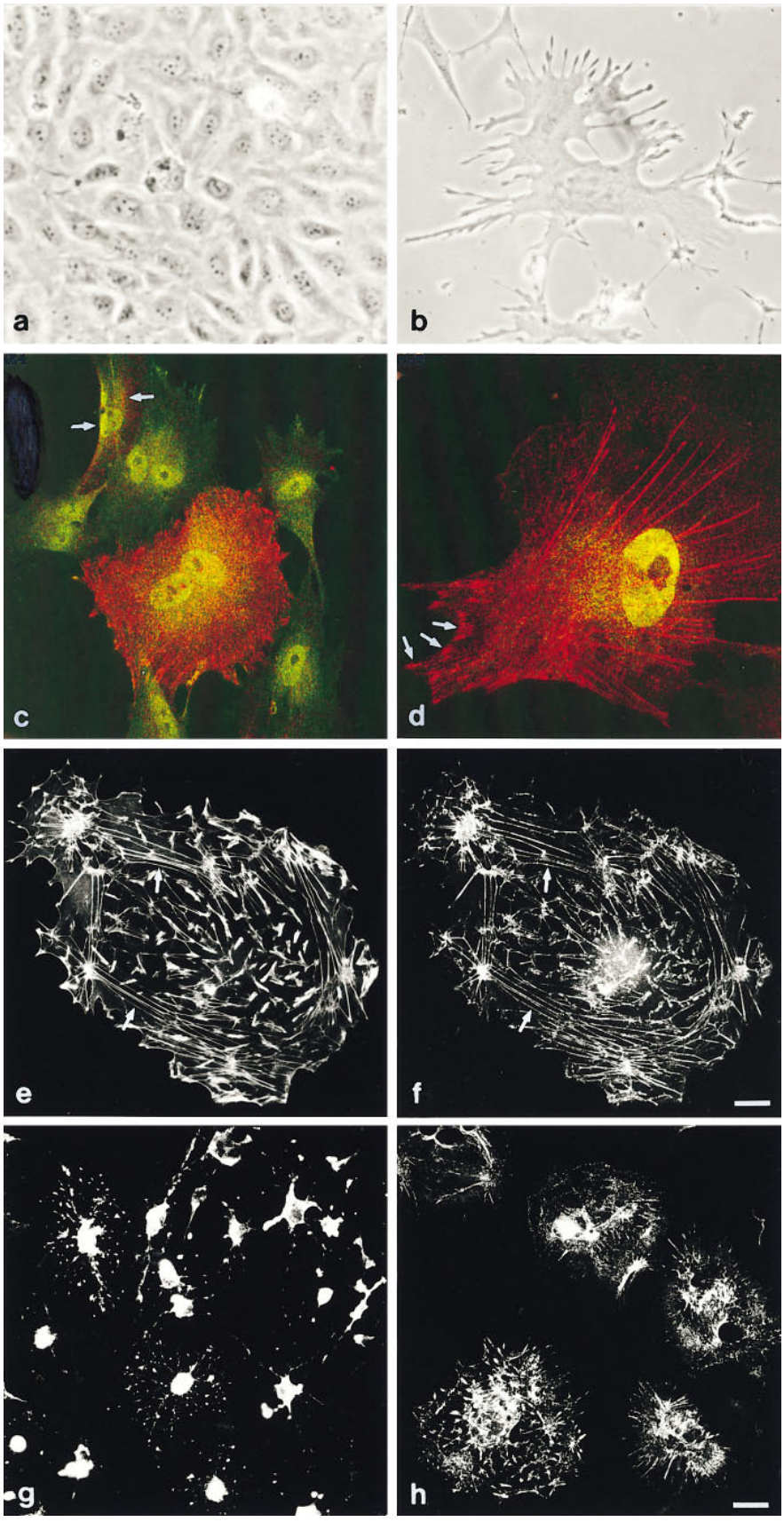

Figure 11. Expression of synaptopodin in a cultured mouse podocyte cell line. (*a*) Phase contrast morphology of undifferentiated podocytes. The cobblestone morphology of undifferentiated podocytes growing under permissive conditions is shown. The cells form a monolayer as they reach confluence. (*b*) Arborized podocytes maintained under nonpermissive conditions are very large and flat. Development of branched processes is obvious. (*c*) Induction of synaptopodin after 4 d at nonpermissive temperature. While all cells express the podocyte-specific transcription factor WT-1 (*green*), cobblestones do not express synaptopodin (*red*). Currently differentiating cells show an induction of synaptopodin (*arrows*). In the center, a differentiated, binucleated, arborized cell is encountered that expresses high levels of synaptopodin. (*d*) Expression of synaptopodin in a differentiated, arborized cell with well developed processes after 14 d at 37°C. Synaptopodin is found along the actin filaments and in focal contacts (*arrows*). The association of synaptopodin with actin was confirmed in double labeling experiments (*e* and *f*) with rhodamin-conjugated phalloidin. (*e*) A linear staining of actin filaments with phalloidin is observed. *f* shows the punctated distribution of synaptopodin along the same actin filaments as in *e* (*arrows*). (*g*) Depolymerization of actin filaments with cytochalasin B abolished the linear staining pattern, and synaptopodin clustered in the perinuclear cytoplasm. (*h*) Depolymerization of microtubules with colcemid did not significantly affect the staining pattern of synaptopodin. Bars, 5 μm.

along the entire molecule, synaptopodin appears virtually as a linear protein without any globular domain structure. This linear conformation may result in a side to side arrangement along the actin microfilaments similar to that recently described for dystrophin (Rybakova et al., 1996). The association of synaptopodin with actin was confirmed in cultured podocytes where the protein colocalized with the microfilaments in a punctate pattern and was also detected in focal contacts. Moreover, after treatment with the actin-depolymerizing drug cytochalasin B, this pattern was abolished. The association with the microfilaments appears to be rather tight, since complete solubilization of synaptopodin can only be achieved by extraction with high salt buffer.

Synaptopodin shares some interesting properties with VASP (Haffner et al., 1995), another proline-rich, actin-associated protein, originally identified due to its phosphorylation upon stimulation of human platelets with cAMP- and cGMP-elevating substances. Like platelets, podocytes also respond to vasodilating substances with alterations of their actin cytoskeleton (for review see Mundel and Kriz, 1995). Like synaptopodin, VASP appears as an elongated, rather linear protein (Haffner et al., 1995). Similar to synaptopodin, which in Western blots shows two bands of 100 and 110 kD, VASP occurs in Western blots as two bands of 46 and 50 kD, with the difference being due to differential phosphorylation (Reinhard et al., 1992). The location at focal adhesions of VASP places it at a site where multiple signals are integrated. This may also be true for synaptopodin, which is found in focal contacts of podocytes. The interactions of VASP with the microfilament system is mediated by profilin (Reinhard et al., 1995). It will be interesting to see whether synaptopodin is a ligand for profilin as well.

Synaptopodin also shares some striking similarities with dendrin, another proline-rich protein whose expression is restricted to dendrites of the forebrain (Herb et al., 1997). While dendrin contains three PPXY motifs, synaptopodin contains two of these PPXY motifs. These motifs are found in several proline-rich proteins and are involved in protein–protein interactions between proline-rich stretches of different proteins and the WW domain (Einbond and Sudol, 1996) as well as the Abl SH3 domain (Bedford et al., 1997) of a variety of proteins. Among others, the WW domain is present in the postsynaptic cytoskeletal proteins dystrophin and utrophin (Bork and Sudol, 1994). Thus, it appears possible that synaptopodin is involved in mediating interactions between actin and associated proteins of the dendritic cytoskeleton.

The distribution of synaptopodin at postsynaptic densities and in dendritc spines is exactly the same as that described for actin in these areas (Matus et al., 1982). Thus, at synapses, as in renal podocytes, synaptopodin colocalizes with actin. One of the most exciting features of synaptopodin is that within the CNS, its expression is restricted to exclusively telencephalic PSD and associated dendritic spines of the olfactory bulb, cerebral cortex, striatum, and hippocampus. In situ hybridization studies, in addition to confirming the exclusive telencephalic expression of synaptopodin, revealed that in contrast to other dendritic proteins like MAP2 (Garner et al., 1988), synaptopodin mRNA is not found in dendrites but in the perikarya only, which may indicidate that synaptopodin synthesis is not controlled locally in the dendritic cytoplasm. As the protein contains potential sites for phosphorylation by protein kinase C, the activity of synaptopodin may be regulated by protein kinase C, which is highly expressed in postsynaptic densities (Cheng et al., 1994) and glomerular podocytes (Cybulsky et al., 1990).

Recently, a novel protein termed striatin was described that, within the telencephalon, also has a prominent expression in dendritic spines (Castets et al., 1996). While both synaptopodin and striatin show similar staining in hippocampus and striatum, in the cerebral cortex, striatin is restricted to the motorcortex, whereas synaptopodin is present in all areas of the cortex. In contrast to synaptopodin, striatin is also found in the cerebellum and the spinal cord; at the subcellular level, synaptopodin is only found in dendrites, whereas striatin is also found in the cell bodies of telencephalic neurons. Since both proteins are only expressed by a subset of dendrites within the hippocampus and striatum, it will be interesting to see whether they define the same synapses in these regions of the brain.

Podocytes of the renal glomerulus are unique cells with a complex cellular organization, consisting of cell body, major processes, and foot processes. From the cell body, major processes arise that directly or after additional branching split into foot processes that interdigitate with the foot processes of neighboring podocytes, leaving in between the filtration slits covered by the slit diaphragm. Like the PSD, the sole plate of podocyte foot processes contains an electron-dense matrix of largely elusive composition (for review see Mundel and Kriz, 1995). The foot processes are equipped with a microfilament-based contractile apparatus composed of actin, myosin II, α actinin, talin, and vinculin, which is linked to the glomerular basement membrane at focal contacts by an $\alpha_3\beta_1$ complex. This contractile apparatus can respond to vasoactive substances with alteration of its actin cytoskeleton and may provide the basis of foot processes motility. In a previous paper, we demonstrated that synaptopodin was not expressed by podocyte precursor cells during nephrogenesis but was first seen as podocytes started to differentiate and develop their typical process architecture (Mundel et al., 1991). At the ultrastructural level, synaptopodin was found to be associated with the actin microfilaments of podocyte foot processes. This association is also seen in vitro, when podocytes transform from simple cobblestone cells into an arborized phenotype equipped with processes similar to those seen in vivo. The late appearance of synaptopodin during postnatal brain development and during differentiation of cultured hippocampal neurons appears to correlate with the maturation of synaptic formations on dendritic spines (Papa et al., 1995; Ziv and Smith, 1996). Thus, at both sites the appearance of synaptopodin appears to be correlated with the formation of cell "processes," which are essential for the specific function of each cell type.

Because of the restricted distribution of synaptopodin, the question arises: which properties are shared by podocyte foot processes and dendritic spines? Podocyte foot processes are able to retract (in extreme forms the result is "foot process effacement") and to spread out again (Shirato et al., 1996), i.e., an individual foot process may decrease or increase in length. Dendritic spine formation and remodelling are crucially involved in what is known as plas-

ticity of the receptor apparatus in the telencephalon (Wallace et al., 1991). Recent work with cultured hippocampal slices (Dailey and Smith, 1996) as well as studies with cultured hippocampal neurons (Papa et al., 1995; Ziv and Smith, 1996) revealed that dendritic filopodia and their protrusive motility may play important roles in initiation and elimination of synaptic contacts, both during development and during postdevelopmental synaptic remodelling processes, such as those representing the morphological basis of long-term memory. Dendritic filopodia seem not only to protrude towards axons but also appear to be able to retract from their axonal counterparts (Ziv and Smith, 1996). Thus, at both sites, in podocyte foot processes as well as in dendritic filopodia and spines, this motility appears to be part of the formation and retraction of cell processes, which may be achieved via the microtubular and actin cytoskeletons (Quinlan and Halpain, 1996). One may speculate that synaptopodin may play a similar function associated with the remodeling of cell processes in the kidney and the CNS. At both sites, these movements and their regulation are poorly understood. Synaptopodin may be a key protein allowing future avenues for the study of these functions.

The conditionally immortal podocyte cell line was established in collaboration with Rolf Zeller (European Molecular Biological Laboratory, Heidelberg, Germany). We gratefully acknowledge the cooperation of Liane Meyn and Carlos Dotti (European Molecular Biological Laboratory) on the studies with cultured hippocampal neurons and of Peter Seeburg (Max Planck Institute for Medical Research, Heidelberg, Germany) on the in situ hybridization studies. We are thankful to H. Spring (German Cancer Research Center) for performing laser scanning confocal microscopy; H.-R. Rackwitz for synthesizing peptides for antibody production; as well as Alexandra Zeller, Stefanie Winter-Simanowski, Andreas Hunziker, Hiltraud Hosser, and Bruni Hähnel for expert technical assistance. We also thank Rolf Nonnenmacher and Ingrid Ertl for skillful artwork and photographical work.

This work was supported by a grant from the Deutsche Forschungsgemeinschaft (Kr 546/9-2).

Received for publication 7 March 1997 and in revised form 10 July 1997.

References

Adler, S. 1992. Characterization of glomerular epithelial cell matrix receptors. *Am. J. Pathol.* 141:571–578.

Bentley, D., and T.P. O'Connor. 1994. Cytoskeletal events in growth cone steering. *Curr. Opin. Neurobiol.* 4:43–48.

Bedford, M.T., D.C. Chan, and P. Leder. 1997. FBP WW domains and the Abl SH3 domain bind to a specific class of proline rich ligands. *EMBO (Eur. Mol. Biol. Organ.) J.* 9:2376–2383.

Bork, P., and M. Sudol. 1994. The WW domain. A signalling site in dystrophin? *Trends Biochem. Sci.* 19:531–533.

Castets, F., M. Bartoli, J.V. Barnier, G. Baillat, P. Salin, A. Moqrich, J.P. Bourgeois, F. Denizot, G. Rougon, G. Calothy, et al. 1996. A novel calmodulin-binding protein, belonging to the WD-repeat family, is localized in dendrites of a subset of CNS neurons. *J. Cell Biol.* 134:1051–1062.

Cheng, G., X.W. Rong, and T.P. Feng. 1994. Block of induction and maintenance of calcium-induced LTP by inhibition of protein kinase C in postsynaptic neuron in hippocampal CA1 region. *Brain Res.* 646:230–234.

Cid-Arregui, A., R.G. Parton, K. Simons, and C.G. Dotti. 1995. Nocodazole-dependent transport, and Brefeldin A-sensitive processing and sorting, of newly synthesized membrane proteins in cultured neurons. *J. Neurosci.* 15:4259–4269.

Cybulsky, A.V., J.V. Bonventre, R.J. Quigg, L.S. Wolfe, and D.J. Salant. 1990. Extracellular matrix regulates proliferation and phospholipid turnover in glomerular epithelial cells. *Am. J. Physiol.* 259:F326–F337.

Dailey, M.E., and S.J. Smith. 1996. The dynamics of dendritic structures in developing hippocampal slices. *J. Neurosci.* 16:2983–2994.

Drenckhahn, D., and R.P. Franke. 1988. Ultrastructural organization of contractile and cytoskeletal proteins in glomerular podocytes of chicken, rat, and man. *Lab Invest.* 59:673–682.

Einbond, A., and M. Sudol. 1996. Towards prediction of cognate complexes between the WW domain and proline-rich ligands. *FEBS (Fed. Eur. Biochem. Soc.) Lett.* 384:1–8.

Garner, C.C., and S. Kindler. 1996. Synaptic proteins and the assembly of synaptic junctions. *Trends Cell Biol.* 6:429–433.

Garner, C.C., R.P. Tucker, and A. Matus. 1988. Selective localization of messenger RNA for cytoskeletal protein MAP2 in dendrites. *Nature (Lond.).* 336:674–677.

Goslin, K., and G. Banker. 1991. Rat hippocampal neurons in low density cultures. *In* Culturing Nerve Cells. G. Banker and K. Goslin, editors. MIT Press, Cambridge, MA. 251–281.

Haffner, C., T. Jarchau, M. Reinhard, J. Hoppe, S.Z. Lohmann, and U. Walter. 1995. Molecular cloning, structural analysis and functional expression of the proline-rich focal adhesion and microfilament associated protein VASP. *EMBO (Eur. Mol. Biol. Organ.) J.* 14:19–27.

Heid, H.W., A. Schmidt, R. Zimbelmann, S. Schäfer, S. Winter-Simanowski, S. Stumpp, M. Keith, U. Figge, M. Schnölzer, and W.W. Franke. 1994. Cell type-specific desmosomal plaque proteins of the plakoglobin family: plakophilin 1 (band 6 protein). *Differentiation.* 58:113–131.

Herb, A., W. Wisden, M.V. Catania, D. Maréchal, A. Dresse, and P.H. Seeburg. 1997. Prominent dendritic localizaiton in forebrain neurons of a novel mRNA and its product, dendrin. *Mol. Cell. Neurosci.* 8:367–374.

Herzog, W., and K. Weber. 1978. Fractionation of brain microtubule-associated proteins. Isolation of two different proteins which stimulate tubulin polymerization in vitro. *Eur. J. Biochem.* 92:1–8.

Jat, P.J., M.D. Noble, P. Ataliotis, Y. Tanaka, N. Yannoutsos, L. Larsen, and D. Kioussis. 1991. Direct derivation of conditionally immortal cell lines from an H-2K^b-tsA58 transgenic mouse. *Proc. Natl. Acad. Sci. USA.* 88:5096–5100.

Kennedy, M.B. 1993. The postsynaptic density. *Curr. Opin. Neurobiol.* 3:732–737.

Kornau, H.-C., L.T. Schenker, M.B. Kennedy, and P.H. Seeburg. 1995. Domain interaction between NMDA receptor subunits and the postsynaptic density protein PSD-95. *Science (Wash. DC).* 269:1737–1740.

Kozak, M. 1989. The scanning model for translation: an update. *J. Cell Biol.* 108:229–241.

Kriz, W. 1996. Progressive renal failure: inability of podocytes to replicate and the consequences for development of glomerulosclerosis. *Nephrol. Dial. Transplant.* 11:1738–1742.

Matus, A., M. Ackermann, G. Pehling, G.R. Byers, and K. Fujiwara. 1982. High actin concentrations in brain synaptic spines and postsynaptic densities. *Proc. Natl. Acad. Sci. USA.* 79:7590–7594.

Monyer, H., R. Sprengel, R. Schoepfer, A. Herb, M. Higuvhi, H. Lomeli, N. Burnashev, B. Sakmann, and P. Seeburg. 1992. Heterodimeric NMDA receptors: molecular and functional distinction of subtypes. *Science (Wash. DC).* 256:1217–1221.

Mundel, P., J. Reiser, A. Zúñiga Mejia Borja, H. Pauenstädt, G.R. Davidson, W. Kriz, and R. Zeller. 1997. Rearrangements of the cytoskeleton and cell contacts induce process formation during differentiation of conditionally immortalized mouse podocyte cell lines. *Exp. Cell Res.* In press.

Mundel, P., and W. Kriz. 1995. Structure and function of podocytes: an update. *Anat. Embryol.* 192:385–397.

Mundel, P., P. Gilbert, and W. Kriz. 1991. Podocytes in glomerulus of rat kidney express a characteristic 44 kD protein. *J. Histochem. Cytochem.* 39:1047–1056.

Mundlos, S., J. Pelletier, A. Darveau, M. Bachmann, A. Winterpacht, and B. Zabel. 1993. Nuclear localization of the protein encoded by the Wims' tumor gene WT1 in embryonic and adult tissues. *Development.* 119:1329–1341.

Papa, M., M.C. Bundman, V. Greenberger, and M. Segal. 1995. Morphological analysis of dendritic spine development in primary cultures of hippocampal neurons. *J. Neurosci.* 12:1–11.

Quinlan, E.M., and S. Halpain. 1996. Postsynaptic mechanisms for bidirectional control of MAP2 phosphorylation by glutamate receptors. *Neuron.* 16:357–368.

Reinhard, M., M. Halbrügge, U. Scheer, C. Wiegand, B.M. Jokusch, and U. Walter. 1992. The 46/50 KD phosphoprotein VASP purified from human platelets is a novel protein associated with actin filaments and focal contacts. *EMBO (Eur. Mol. Biol. Organ.) J.* 11:2063–2070.

Reinhard, M., K. Giehl, K. Abel, C. Haffner, T. Jarchau, V. Hoppe, B.M. Jokusch, and U. Walter. 1995. The proline-rich focal adhesion and microfilament protein VASP is a ligand for profilins. *EMBO (Eur. Mol. Biol. Organ.) J.* 14:1583–1589.

Rosenmund, C., and G.L. Westbrook. 1993. Calcium-induced actin depolymerization reduces NMDA channel activity. *Neuron.* 10:805–814.

Rybakova, I.N., K.J. Amann, and J.M. Ervast. 1996. A new model for the interaction of dystrophin with F-actin. *J. Cell Biol.* 135:661–672.

Schäfer, S., P.J. Koch, and W.W. Franke. 1994. Identification of the ubiquitous human desmoglein, Dsg2, and the expression catalogue of the desmoglein subfamily of desmosomal cadherins. *Exp. Cell Res.* 222:269–274.

Sheng, M. 1996. PDZs and receptor/channel clustering: rounding up the latest suspects. *Neuron.* 17:575–578.

Shirato, I., T. Sakai, K. Kimura, Y. Tomino, and W. Kriz. 1996. Cytoskeletal changes in podocytes associated with foot process effacement in Masugi nephritis. *Am. J. Pathol.* 148:1283–1296.

Wallace, C., N. Hawrylak, and W.T. Greenough. 1991. Studies of synaptic structural modifications after long-term potentiation and kindling: context for a molecular morphology. *In* Long-Term Potentiation: A Debate of Current Issues. M. Baudry and J.L. Davis, editors. MIT Press, Cambridge, MA. 189–232.

Wyszynski, M., J. Lin, A. Rao, E. Nigh, A.H. Beggs, A.M. Craig, and M. Sheng. 1997. Competitive binding of α actinin and calmodulin to the NMDA receptor. *Nature (Lond.).* 385:439–442.

Ziv, N.E., and S.J. Smith. 1996. Evidence for a role of dendritic filopodia in synaptogenesis and spine formation. *Neuron.* 17:91–102.